A 94-GHz Aperture-Coupled Micromachined Microstrip Antenna

Gildas P. Gauthier, *Student Member, IEEE*, Jean-Pierre Raskin, *Member, IEEE*, Linda P. B. Katehi, *Fellow, IEEE*, and Gabriel M. Rebeiz, *Fellow, IEEE*

***Abstract*— This paper presents an aperture-coupled micromachined microstrip antenna operating at 94 GHz. The design consists of two stacked silicon substrates: 1) the top substrate, which carries the microstrip antenna, is micromachined to improve the radiation performance of the antenna and 2) the bottom substrate, which carries the microstrip feed line and the coupling slot. The measured return loss is −18 dB at 94 GHz for a 10-dB bandwidth of 10%. A maximum efficiency of 58 ± 5% has been measured and the radiation patterns show a measured front-to-back ratio of −10 dB at 94 GHz. The measured mutual coupling is below −20 dB in both E- and H-plane directions due to the integration of small 50-μm silicon beams between the antennas. The micromachined microstrip antenna is an efficient solution to the vertical integration of antenna arrays at millimeter-wave frequencies.**

***Index Terms*— Micromachining, microstrip antennas, millimeter-wave antennas.**

I. Introduction

THE microstrip antenna is a very good common element in telecommunication and radar applications since it provides a wide variety of designs, can be planar or conformal, and can be fed in many different methods [1], [2]. It is also compact and suitable for antenna array designs. Microstrip antennas can be used in applications which requires high-performance compact low-cost planar antennas such as imaging arrays and collision-avoidance radars. The aperture-coupled microstrip antenna [3], [4] is of great interest since it allows for the electromagnetic separation of the radiating element (the microstrip patch) and the feed network with the use of the ground plane. At millimeter-wave frequencies, many limitations have to be overcome in order to design high-performance microstrip antennas on silicon or GaAs substrates.

The high dielectric constant of the substrates used ($\epsilon_r = 11.7$ for silicon) implies that surface waves are more easily triggered in the substrate. The power lost to surface waves can be reduced by using thin substrates, typically $\lambda_d/10$, where λ_d is the dielectric wavelength. At 94 GHz for silicon, it corresponds to around 100-μm-thick substrates. However, while it is possible to design good RF circuits on thin high-dielectric constant substrates, the radiation efficiency of microstrip antennas will be greatly reduced.

A recent solution is the use of micromachining fabrication techniques to artificially remove the substrate below the antenna and, therefore, locally synthesize a low-dielectric constant region around the antenna. This technique has been successfully applied by drilling closely spaced holes [5] or a cavity around and beneath the microstrip antenna [6]. Also, a low-loss transition from microstrip to coplanar waveguide (CPW) transmission line must be designed so as to integrate the microstrip antenna in a configuration where the feed network is CPW based.

Manuscript received December 16, 1998; revised September 23, 1999. This work was supported by Hughes/DARPA, under Contract FR-573420-SR8.

G. P. Gauthier, L. P. B. Katehi, and G. M. Rebeiz are with the Electrical Engineering and Computer Science Department, The University of Michigan, Ann Arbor, MI 48109-2122 USA.

J.-P. Raskin was with the Electrical Engineering and Computer Science Department, The University of Michigan, Ann Arbor, MI 48109-2122 USA. He is now with the Microwave Laboratory, Université Catholique de Louvain, Louvain-la-Neuve, B-1348 Belgium.

Publisher Item Identifier S 0018-926X(99)09976-7.

II. Antenna Design

Fig. 1 shows the perspective view and the cross section of the aperture-coupled micromachined microstrip antenna. The design of the antenna is summarized below (referring to Fig. 2).

A. Antenna

A cavity is etched in the substrate below the microstrip antenna. The synthesized effective dielectric constant (ϵ_{eff}) is characterized to determine the antenna dimensions (W, L) for a resonance at 94 GHz. The effective dielectric constant is the quasistatic value seen underneath the microstrip patch antenna and is in the range of 2.8–3.9, depending on the etching depth. The antenna is analyzed using the cavity model and the effective dielectric constant. There are no models describing the effect of the cavity width and this will be the object of a further study. We believe that the cavity around the antenna can be designed to resonate close to the microstrip antenna resonance and, therefore, resulting in an increase in bandwidth [5].

The influence of the slot shape has been studied previously by Pozar and Rathi [7], [8]. A H-shaped slot (Fig. 2) is used, which improves the coupling compared to a rectangular slot. The H-slot design results in a short slot and pushes the resonant frequency of the slot above that of the microstrip antenna, thereby improving the front-to-back ratio. The real part of the aperture-coupled microstrip antenna input impedance is fixed by the length of the slot L_s and is designed to be 50 Ω. The imaginary part of the aperture-fed microstrip antenna input impedance is then compensated by the microstrip line extension L_{st}, which acts like a matching stub (Fig. 2). The

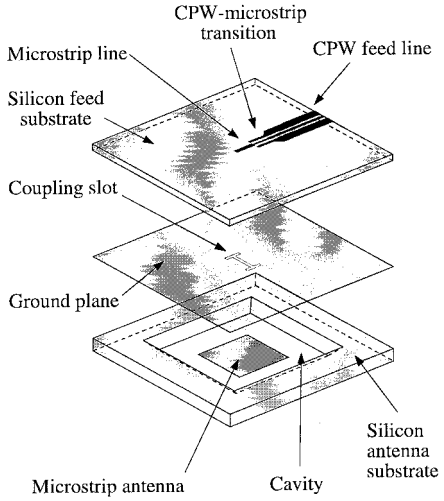

Fig. 1. (a) Perspective view and (b) cross section of the aperture-coupled micromachined microstrip antenna. All dimensions are in microns.

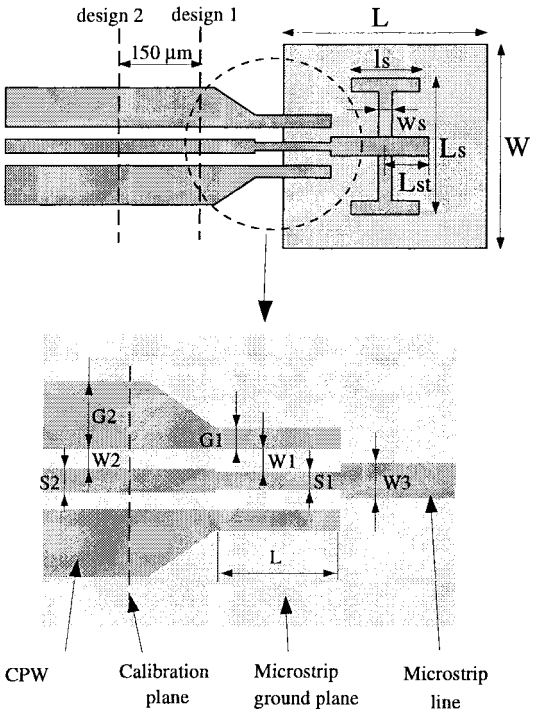

Fig. 2. Top view of the microstrip antenna design and of the CPW-to-microstrip transition.

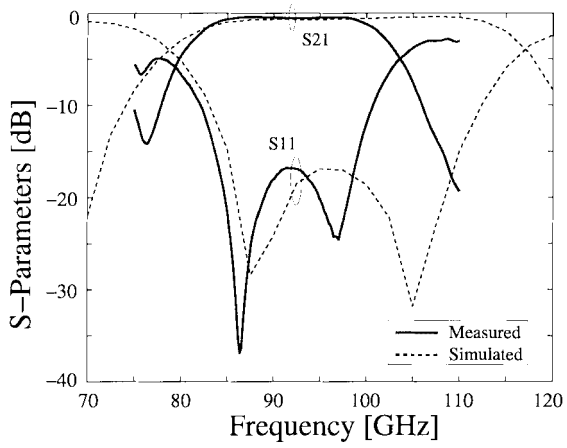

Fig. 3. Measured and simulated (IE3D) performance of the CPW-to-microstrip transition.

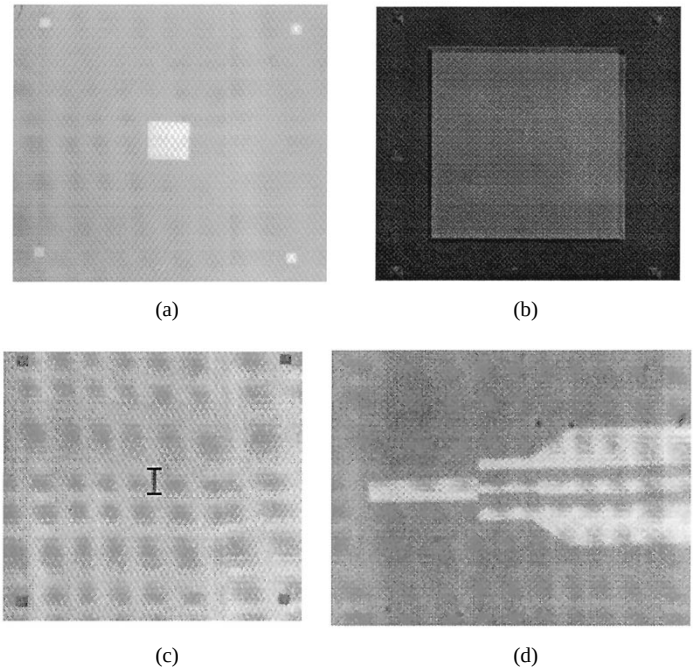

Fig. 4. (a) Pictures of the microstrip antenna, (b) micromachined cavity, (c) coupling-slot, and (d) feed line. The four pictures are not at the same scale.

simulation is done using a commercial analysis program IE3D (Zeeland Software [9]).

B. CPW to Microstrip Line Transition

In order to integrate the microstrip antenna in an array where the feed network is based on CPW lines, a simple low-loss, and compact CPW to microstrip transition is designed, extending the work of Houdard *et al.* [10] at W-band frequencies. It can be analyzed as a three-line microstrip coupler and more details can be found in [11]. Fig. 2 shows the layout and, Fig. 3 shows the measured and simulated performance of the transition used at W-band frequencies. The FGCPW feed-line dimensions are $S_2 = 40$ μm, $W_2 = 24$ μm, and $G_2 = 106$ μm corresponding to a chatacteristic impedance

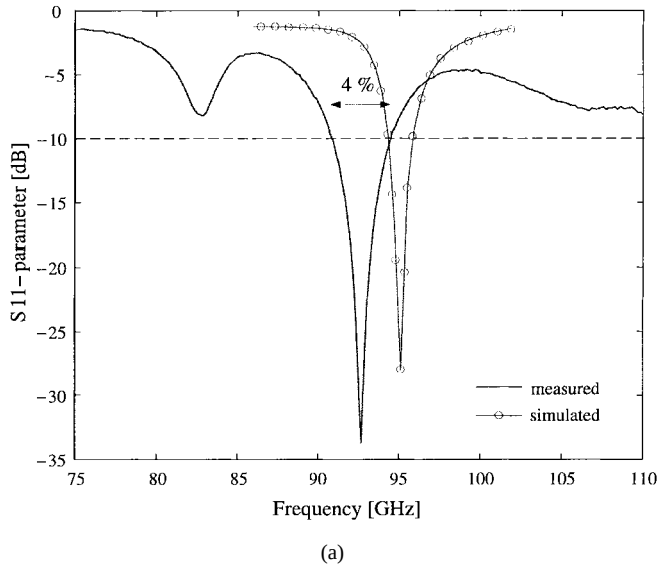

(a)

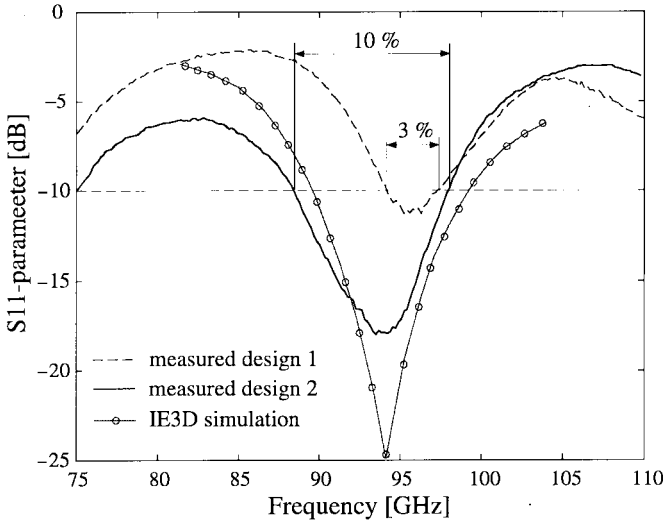

(b)

Fig. 5. (a) Measured and simulated (IE3D) input impedance of the microstrip antenna built on a full silicon substrate of 100 μm thick and (b) on a 200-μm-thick silicon wafer in which a 150-μm-deep cavity has been etched.

of 50 Ω. The microstrip line is $W_3 = 74$ μm wide resulting in a 50-Ω characteristic impedance. The dimensions of the CPW-to-microstrip transition are $S_1 = 30$ μm, $W_1 = 29$ μm, and $G_1 = 45$ μm. The coupling region is chosen to be $L = 280\mu$m long ($\lambda_d/4$ at 94 GHz). A back-to-back transition separated by a 860μm long microstrip line results in 0.2 dB insertion loss per transition with a bandwidth of 20%. The return loss is better than -17 dB from 85 to 100 GHz.

III. Input Impedance

Two aperture-coupled microstrip antennas are designed for 94-GHz operation. One is built on a full 100-μm-thick silicon wafer and the other on a 200-μm-thick silicon wafer in which a 150 μm deep cavity has been etched using tetramethyl ammonium hydroxide (TMAH) or potassium hydroxide (KOH)

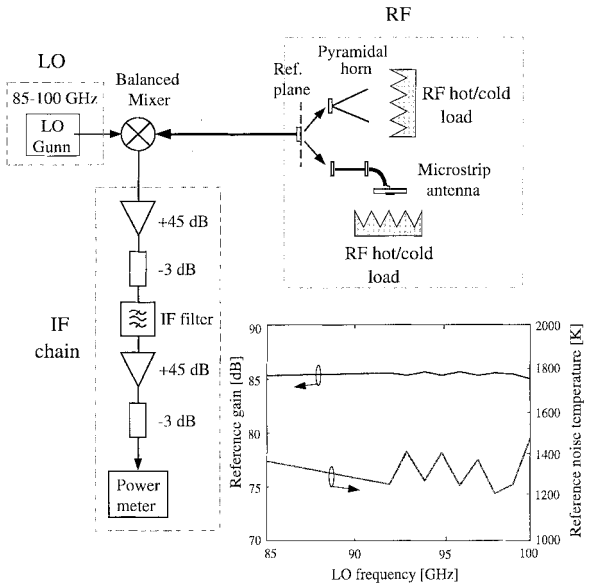

Fig. 6. Radiometric measurement setup at 85–100 GHz.

wet-etching techniques [12]. Referring to Figs. 1 and 2, the antenna and slot dimensions are, respectively, $W \times L = 380$ μm $\times$ 380 μm and $L_s \times l_s \times w_s = 270$ μm $\times$ 120 μm $\times$ 50 μm for the antenna integrated on a full silicon wafer of 100 μm thick and $W \times L = 800$ μm $\times$ 800 μm and $L_s \times l_s \times w_s = 500$ μm $\times$ 250 μm $\times$ 50 μm for the micromachined microstrip antenna. The bottom silicon substrate is identical for both designs and is 100 μm thick (feedline substrate). The microstrip line is $W_3 = 74$ μm wide resulting in a 50-Ω characteristic impedance and the matching stub is $L_{st} = 250$ μm long for the nonmicromachined antenna and $L_{st} = 160$ μm long for the micromachined one. The CPW feed line and the CPW-to-microstrip transition used for coplanar-probe on-wafer measurements are the same for the micromachined and the nonmicromachined antennas. The dimensions of these are given in Section II-B. All metal layers are 8000 Å of evaporated gold, corresponding to around three skin depths at 94 GHz. Fig. 4 shows the pictures of the antenna, cavity, slot and feed line for the aperture-coupled micromachined microstrip antenna.

The input impedance of the two antennas is measured using W-band picoprobes on a HP8510 network analyzer and TRL calibration is used to move the reference plane from the probe-tip to the plane shown in Fig. 2. The simulated (IE3D) and measured input impedances of both microstrip antennas are shown in Fig. 5. It is seen that there is a 2.5% frequency shift between the measured and simulated response, which could be attributed to small variations in the silicon wafer thickness, and to the general inaccuracies of numerical packages in high Q ($\epsilon_r = 11.7$) structures at millimeter-wave frequencies (probably due to the simulation at the exact current distribution in the slot feed). A return loss of -35 dB at 92.5 GHz with a 10-dB bandwidth of 4% has been measured for the antenna built on a full silicon wafer of 100 μm thick. Also, a return loss of -12 dB at 95 GHz with a 10-dB bandwidth of 3% and of -18 dB at 94 GHz with a 10-dB

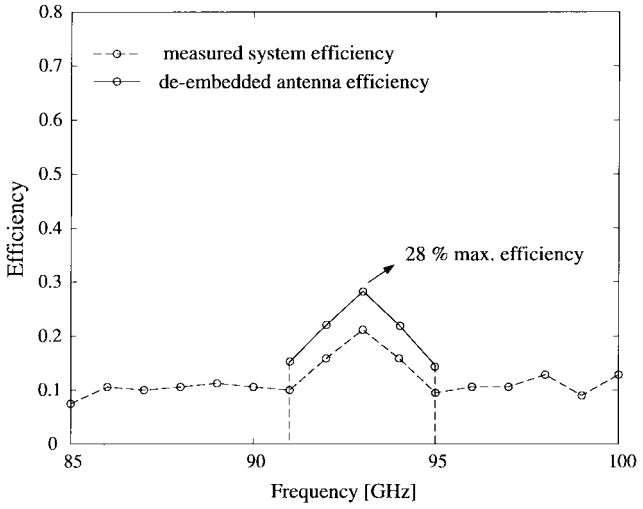

(a)

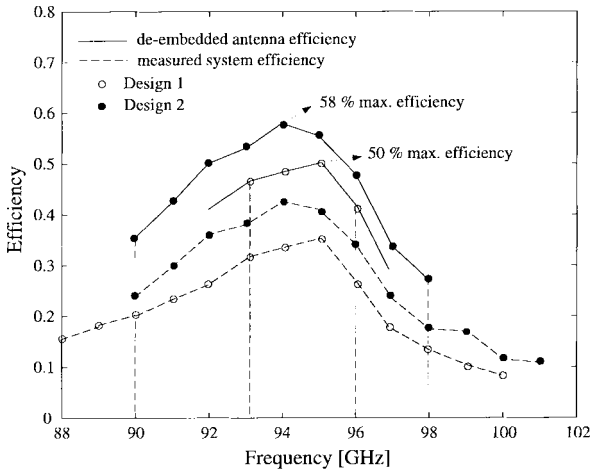

(b)

Fig. 7. (a) Measured radiation efficiency of a microstrip patch antenna built on a full 100-μm silicon wafer and (b) of a micromachined microstrip antenna.

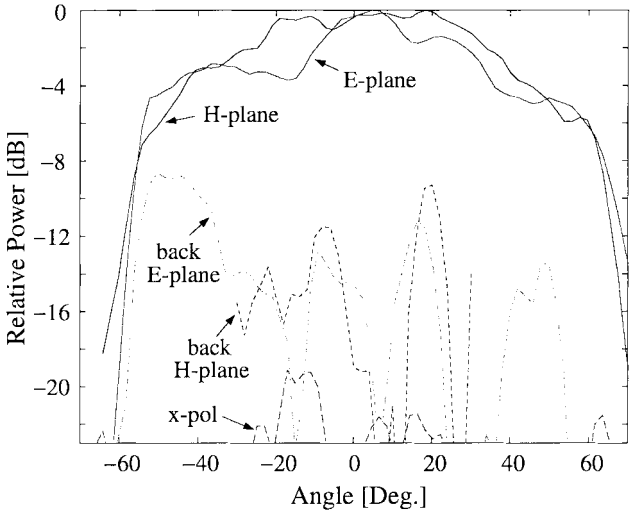

Fig. 8. Measured radiation patterns of the micromachined microstrip antenna at 94 GHz.

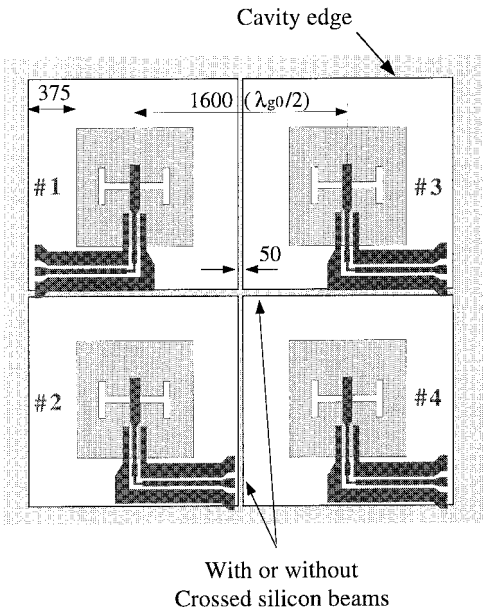

Fig. 9. Layout of the 2 × 2 antenna array to measure the mutual coupling. All dimensions are in microns.

bandwidth of 10% has been obtained for the micromachined microstrip antenna, respectively, for designs 1 and 2. Notice that in this case, the simulation agrees very well with the measurement due to the low Q ($\epsilon_r = 3.0$) nature of the micromachined antenna. The only difference between designs 1 and 2 in Fig. 5(b) is the length of the input CPW feed line, which is around 150 μm. The important variation of the antenna return loss for the two different designs can be explained by the dependence of the CPW-to-microstrip transition versus the length of the CPW feed line. This dependence is attributed to a parasitic microstrip mode, which is triggered by the transition discontinuity and propagating along the coplanar ground planes of the conductor-backed CPW feed line. The conversion mode at discontinuities in conductor-backed CPW has been shown by Jackson in [13]. Various back-to-back CPW-to-microstrip transitions has been designed and measured to fully characterize the parasitic microstrip mode along the conductor-backed feed CPW line and to cancel it. These experimental results are out of the scope of this article and will be presented in another publication [14].

IV. Radiation Efficiency

The radiometric technique is an accurate method to measure the radiation efficiency of planar antennas using standard hot/cold load measurements. The microstrip antenna is connected to a calibrated (low-noise) system of gain G_s and noise temperature T_s. The RF chain is calibrated using a standard WR-10 pyramidal horn which has a known radiation efficiency of 97–98%. The horn is then replaced by the microstrip antenna connected to the chain via a W-band picoprobe. This method is a double side-band (DSB) measurement since no RF filter is used to separate the upper side-band from the lower side-band before mixing down to the intermediate frequency (IF). The measurement is, therefore, more accurate if a small IF is chosen (see [5] for more details). A detailed view of the RF chain is shown in Fig. 6. The conversion loss of the W-

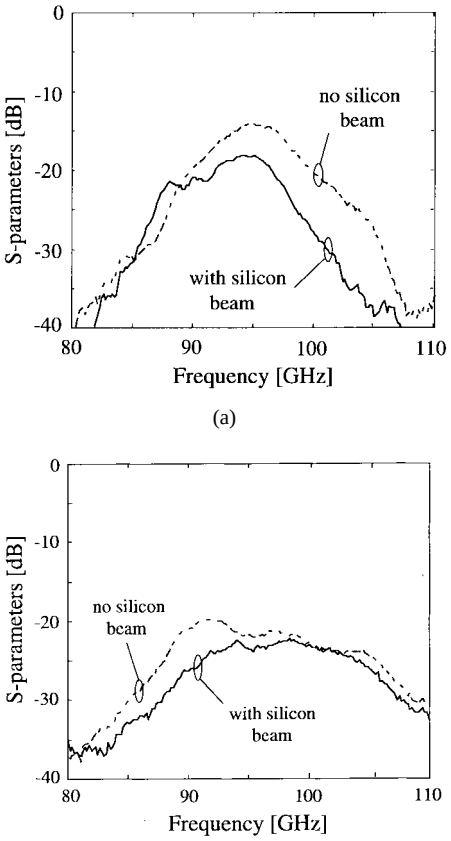

Fig. 10. Measured mutual coupling comparison in the (a) E- and (b) H-plane directions.

band balanced mixer is 8 dB over the 80–100 GHz bandwidth. The IF is fixed at 200 MHz. The calibrated IF chain has a gain of 86 dB and a noise temperature of 111 K. The total system DSB noise temperature and gain are equal to around 1500 K and 86 dB, respectively (Fig. 6).

Fig. 7 represents the measured radiation efficiency of different designed microstrip antennas using the radiometric method. The measured radiation efficiency improved from $27 \pm 5\%$ for the 100-μm-thick silicon substrate $(\epsilon_r = 11.7)$ to $58 \pm 5\%$ (design 2) for the micromachined antenna with $\epsilon_{eff} = 3.0$. Notice that design 1 resulted in 50% radiation efficiency due to some power loss in the CPW-to-microstrip transition. The dashed curves in Fig. 7 represent the measurement results including the microprobe losses (1.0 dB), the feedline losses (0.2 dB), and the mismatch loss to 50-Ω load. The straight lines represent the de-embedded radiation efficiency of microstrip antenna designs around their resonant frequency.

V. Radiation Patterns

To measure the radiation patterns of the micromachined microstrip antenna, a bismuth bolometer is integrated into the circuit. The RF short in the CPW line is provided by a thin-film capacitor (300 μm $\times$ 200 μm $\times$ 1500 Å of evaporated SiO). Two 100-Ω bismuth bolometers (4 μm $\times$ 4 μm and 1000 Å thick) are placed in parallel $\lambda_g/4$ away from the RF short (where λ_g is the guided wavelength in the CPW line) and result in a 50-Ω bolometer resistance.

The measured radiation patterns are shown in Fig. 8 and are typical for microstrip antennas. It is seen that the cross-polarization level is below -20 dB and the front-to-back ratio is below -10 dB for both E- and H-plane directions. The ripples in the E-plane are due to the finite ground of the microstrip antenna (3×3 λ_0).

This microstrip-type antenna has an excellent a 10-dB bandwidth (10%), good patterns, and high-efficiency performance and is compatible with silicon or GaAs MMIC technology.

Two different 2×2 micromachined antenna arrays with a spacing of $0.5\lambda_0$ have been built to measure the mutual coupling between patches in the E- and H-plane directions. The shape of the cavity etched underneath patches is the only parameter modified between the two designs. In one case, only one wide cavity underneath the four microstrip antennas (Fig. 9) is used. In the other case, an individual cavity for each patch separated by a 50-μm-wide silicon beam is used. The crosstalk in E- and H-plane directions is measured using W-band picoprobes on a HP8510 network analyzer. Fig. 10 shows that crossed silicon beams reduce the parasitic mutual coupling in the two main plane directions to less than -20 dB. This coupling level is sufficiency low to design very efficient antenna arrays in W-band.

References

[1] I. J. Bahl and P. Bhartia, *Microstrip Antennas*. Dedham, MA: Artech House, 1982.
[2] J. R. James and P. S. Hall, *Handbook of Microstrip Antennas*. London, U.K.: Peregrinus, 1989.
[3] D. M. Pozar, "A microstrip antenna aperture coupled to a microstripline," *Electron. Lett.*, vol. 21, no. 2, pp. 49–50, Jan. 1985.
[4] P. L. Sullivan and D. H. Schaubert, "Analysis of an aperture coupled microstrip antenna," *IEEE Trans. Antennas Propagat.*, vol. 34, pp. 977–984, Aug. 1986.
[5] G. P. Gauthier, A. Courtay, and G. M. Rebeiz, "Microstrip antennas on synthesized low dielectric-constant substrates," *IEEE Trans. Antennas Propagat.*, vol. 45, pp. 1310–1314, Aug. 1997.
[6] J. P. Papapolymerou, R. F. Drayton, and L. P. B. Katehi, "Micromachined patch antennas," *IEEE Trans. Antennas Propagat.*, vol. 46, pp. 275–283, Feb. 1998.
[7] D. M. Pozar and S. D. Targonski, "Improved coupling for aperture coupled microstrip antennas," *Electron. Lett.*, vol. 27, no. 13, pp. 1129–31, June 1991.
[8] V. Rathi, G. Kumar, and K. P. Ray, "Improved coupling for aperture coupled microstrip antennas," *IEEE Trans. Antennas Propagat.*, vol. 44, pp. 1196–1198, Aug. 1996.
[9] IE3D Version 4, Zeland Software, Inc., Fermont, CA, 1994.
[10] M. Houdart and C. Aury, "Various excitation of coplanar waveguide," in *IEEE-MTT Int. Microwave Symp. Dig.*, Orlando, FL, May 1979, pp. 116–118.
[11] G. P. Gauthier, L. P. Katehi, and G. M. Rebeiz, "W-band finite ground coplanar waveguide (FGCPW) to microstrip line transition," in *IEEE-MTT Int. Microwave Symp. Dig.*, Baltimore, MD, June 1998, pp. 107–109.
[12] K. E. Peterson, "Silicon as a mechanical material," *Proc. IEEE*, vol. 70, pp. 420–457, May 1982.
[13] R. W. Jackson, "Mode conversion at discontinuities in finite-width conductor-backed coplanar waveguide," *IEEE Trans. Microwave Theory Tech.*, vol. 37, pp. 1582–1589, Oct. 1989.
[14] J.-P. Raskin, G. P. Gauthier, L. P. Katehi, and G. M. Rebeiz, "Mode conversion at CPW-to-microstrip transition discontinuities," *IEEE Trans. Microwave Theory Tech.*, to be published.

Gildas P. Gauthier (S'96) was born in Angers, France, in 1969. He received the Dipl. (telecommunications engineer) and DEA degrees from ENST Bretagne, Brest, France, in 1992 and 1993, respectively, and the Ph.D. degree in electrical engineering from The University of Michigan, Ann Arbor, in 1999.

He is currently with at Thomson-CSF Microelectronics, Paris, France.

Jean-Pierre Raskin (M'97) was born in Aye, Belgium, in 1971. He received the Industrial Engineer degree from the Institut Supérieur Industriel d'Arlon, Belgium, in 1993, and the B.S. and Ph.D. degrees in applied sciences from the Université Catholique de Louvain, Louvain-la-Neuve, Belgium, in 1994 and 1997, respectively.

From 1994 to 1997, he was a Research Engineer at the Laboratoire d'Hyperfréquences, Université Catholique de Louvain, Belgium. He worked on the modeling, characterization and realization of monolithic microwave integrated circuits in silicon-on-insulator technology for low-power low-voltage applications. In 1998 he joined the Electrical Engineering and Computer Science Department, The University of Michigan, Ann Arbor. His current research involves the development and characterization of micromachining fabrication techniques for microwave and millimeter-wave circuits and microelectromechanical transducers/amplifiers working in hard environments.

Linda P. B. Katehi (S'81–M'84–SM'89–F'95) received the B.S.E.E. degree from the National Technical University of Athens, Greece, in 1977, and the M.S.E.E. and Ph.D. degrees from the University of California, Los Angeles, in 1981 and 1984, respectively.

In September 1984, she joined the faculty of the Electrical Engineering Computer Science Department, University of Michigan, Ann Arbor, where she is currently an Associate Dean for graduate education and a Professor of electrical engineering and computer science. She has been interested in the development and characterization (theoretical and experimental) of microwave, millimeter-printed circuits, computer-aided design of very large scale integration interconnects, the development and characterization of micromachined circuits for millimeter-wave and submillimeter-wave applications, and the development of low-loss lines for Terahertz-frequency applications. She has also been studying, theoretically and experimentally, various types of uniplanar radiating structures for hybrid and monolithic circuits, as well as monolithic oscillator and mixer designs.

Dr. Katehi was awarded the IEEE AP-S W. P. King (Best Paper Award for a Young Engineer) in 1984, the IEEE AP-S S. A. Schelkunoff Award (Best Paper Award) in 1985, the NSF Presidential Young Investigator Award in 1987, the URSI Young Scientist Fellowship in 1987, the Humboldt Research Award and The University of Michigan Faculty Recognition Award in 1994, the IEEE MTT-S Microwave Prize in 1996, and the 1997 Best Paper Award from the International Society on Microelectronics and Advanced Packaging. She is a member of IEEE AP-S, MTT-S, Sigma XI, Hybrid Microelectronics, URSI Commission D, and a member of AP-S ADCOM (1992 to 1995). She is also an Associate Editor for the IEEE TRANSACTIONS ON MICROWAVE THEORY AND TECHNIQUES.

Gabriel M. Rebeiz (S'86–M'88–SM'93–F'97) received the Ph.D. degree in electrical engineering from the California Institute of Technology, Pasadena, in June 1988.

He joined the faculty of The University of Michigan, Ann Arbor, in September 1988 and was promoted to Full Professor in May 1998. He has held short visiting professorships at Chalmers University of Technology, Gothenburg, Sweden, École Normale Supérieure, Paris, France, and Tohoku University, Sendai, Japan. His research interests include applying micromachining techniques and microelectromechanical systems (MEMS) for the development of novel components and subsystems for wireless communication systems. He is also interested in Si/GaAs RFIC design for receiver applications and in the development of planar antennas and microwave/millimeter-wave front-end electronics for applications in millimeter-wave communication systems, automotive collision-avoidance sensors, monopulse tracking systems, and phased arrays.

Dr. Rebeiz received the National Science Foundation Presidential Young Investigator Award in April 1991 and the URSI International Isaac Koga Gold Medal Award for Outstanding International Research in August 1993. He also received the Research Excellence Award in April 1995 from the University of Michigan. Together with his students, he is the winner of Best Student Paper Awards at IEEE-MTT (1992, 1994–1999), and IEEE-AP (1992 and 1995). He received the JINA 1990 Best Paper Award. He received the EECS Department Teaching Award in October 1997, the College of Engineering Teaching Award in May 1998, and was selected by the students as the 1997–1998 Eta-Kappa-Nu EECS Professor of the Year. In June 1998, he received the Amoco Foundation Teaching Award, given yearly to one (or two) faculty at the University of Michigan for excellence in undergraduate teaching.